Received: 1 August 2023 | Revised: 20 December 2023 | Accepted: 26 December 2023

DOI: 10.1096/fj.202301557RR

RESEARCH ARTICLE

The FASEB Journal

The sphingosine-1-phosphate receptor 1 modulator ponesimod repairs cuprizone-induced demyelination and induces oligodendrocyte differentiation

Emily Willems[1,2] | Melissa Schepers[1,2,3] | Elisabeth Piccart[1] | Esther Wolfs[4] | Niels Hellings[3,5] | Maria Ait-Tihyaty[6] | Tim Vanmierlo[1,2,3]

[1]Department of Neuroscience, Biomedical Research Institute, Faculty of Medicine and Life Sciences, Hasselt University, Diepenbeek, Belgium

[2]Department Psychiatry and Neuropsychology, School for Mental Health and Neuroscience, Maastricht University, Maastricht, Netherlands

[3]University MS Center (UMSC) Hasselt-Pelt, Hasselt, Belgium

[4]Department of Cardio and Organ Systems, Biomedical Research Institute, Hasselt University, Diepenbeek, Belgium

[5]Department of Immunology and Infection, Biomedical Research Institute, Hasselt University, Diepenbeek, Belgium

[6]Janssen Research & Development, LLC, Titusville, New Jersey, USA

Correspondence
Tim Vanmierlo, Department of Neuroscience, Biomedical Research Institute, Faculty of Medicine and Life Sciences, Hasselt University, Diepenbeek, Belgium.
Email: tim.vanmierlo@uhasselt.be

Abstract

Sphingosine-1-phosphate receptor (S1PR) modulators are clinically used to treat relapse-remitting multiple sclerosis (MS) and the early phase of progressive MS when inflammation still prevails. In the periphery, S1PR modulators prevent lymphocyte egress from lymph nodes, hence hampering neuroinflammation. Recent findings suggest a role for S1PR modulation in remyelination. As the Giα-coupled S1P1 subtype is the most prominently expressed S1PR in oligodendrocyte precursor cells (OPCs), selective modulation (functional antagonism) of S1P1 may have direct effects on OPC functionality. We hypothesized that functional antagonism of S1P1 by ponesimod induces remyelination by boosting OPC differentiation. In the cuprizone mouse model of demyelination, we found ponesimod to decrease the latency time of visual evoked potentials compared to vehicle conditions, which is indicative of functional remyelination. In addition, the Y maze spontaneous alternations test revealed that ponesimod reversed cuprizone-induced working memory deficits. Myelin basic protein (MBP) immunohistochemistry and transmission electron microscopy of the corpus callosum revealed an increase in myelination upon ponesimod treatment. Moreover, treatment with ponesimod alone or in combination with A971432, an S1P5 monoselective modulator, significantly increased primary mouse OPC differentiation based on O4 immunocytochemistry. In conclusion, S1P1 functional antagonism

Abbreviations: BSA, bovine serum albumin; cAMP, cyclic adenosine monophosphate; cDNA, complement deoxyribonucleic acid; CO_2, carbon dioxide; DAPI, 4′,6-diamidino-2-phenylindole; DMEM, Dulbecco's modified eagle medium; DMSO, dimethyl sulfoxide; ERK, extracellular signal-regulated kinases; FDA, food and drug administration; FGF, fibroblast growth factor; FTY720, fingolimod; GFAP, glial fibrillary acidic protein; ICC, immunocytochemistry; IHC, immunohistochemistry; MAPK, mitogen-activated protein kinase; MBP, myelin basic protein; MMPs, matrix metalloproteinases; mRNA, messenger ribonucleic acid; MS, multiple sclerosis; NG2, neuron glial 2; OPC, oligodendrocyte precursor cell; PBS, phosphate-buffered saline; PBS-T, phosphate-buffered saline with tween20; PCR, polymerase chain reaction; PDGF, platelet-derived growth factor; P-FTY720, fingolimod-phosphate; qPCR, quantitative polymerase chain reaction; ROCK, Rho-associated protein kinase; RRMS, relapse-remitting multiple sclerosis; S1P, sphingosine-1-phosphate; S1P1, sphingosine-1-phosphate receptor 1; S1P3, sphingosine-1-phosphate receptor 3; S1P4, sphingosine-1-phosphate receptor 4; S1P5, sphingosine-1-phosphate receptor 5; S1PR, sphingosine-1-phosphate receptor; SEM, standard error of the mean; SPMS, secondary progressive multiple sclerosis; TEM, transmission electron microscopy; USA, United States of America; VEP, visual evoked potential.

Funding information
Janssen Research and Development (JRD)

by ponesimod increases remyelination in the cuprizone model of demyelination and significantly increases OPC differentiation in vitro.

KEYWORDS
cuprizone, multiple sclerosis, oligodendrocyte precursor, remyelination, visual evoked potentials

1 | INTRODUCTION

With approximately 2.8 million people affected worldwide, multiple sclerosis (MS) is one of the most prevalent neurodegenerative diseases among young adults.[1,2] MS is characterized by immune cell infiltration and subsequent degradation of the axonal myelin sheath.[3] Modulation of sphingosine-1-phosphate receptors (S1PR) has become a widely applied treatment option for immune active MS. S1PR are a family of G-protein-coupled receptors, with five identified subtypes (S1P1–5).[4] Four oral S1PR modulating agents, that cause receptor internalization and subsequent degradation (functional antagonism), have been FDA-approved in relapsing-remitting MS (RRMS) treatment strategies. These agents, of which fingolimod (FTY720) was the first S1PR modulator to be approved in 2010, prevent T-cell egression from secondary lymph organs.[5] Later, modulators with an S1PR subtype selectivity, such as the dual S1P1/S1P5 selective modulators siponimod (Mayzent, Novartis©) and ozanimod (Zeposia, Celgene©), were approved for RRMS and active secondary progressive MS (SPMS).[6–9] These cell-trafficking inhibitors are mainly used as immunomodulating agents in RRMS. However, the failure of endogenous remyelination in progressive MS remains an unmet need and hence prime therapeutic focus. As >35% of RRMS patients eventually develop SPMS within 10 years, there is a vast therapeutic need.[10] Whereas the differentiation of oligodendrocyte precursor cells (OPCs) into mature oligodendrocytes in RRMS correlates with periods of remission, this differentiation capacity is largely lost when the disease progresses.[11] Upon demyelination, immature OPCs migrate to the lesion site and subsequently differentiate toward mature myelinating oligodendrocytes.[12] When OPC differentiation is hampered, as seen in SPMS, remyelination fails, and phases of remission are less prominent leading to chronic disease progression.[13] Hence, agents that directly stimulate OPC differentiation are predicted to be promising in halting disease progression. Since OPCs express all S1PR except S1P4, and S1PR modulation affects pathways involved in migration and cell maturation, a role for S1PR modulation in remyelination is suggested.[14] Previously, oral treatment with siponimod (dual S1P1 and S1P5) has been shown to improve remyelination in a cuprizone model. FTY720 (non-selective) and ozanimod (dual S1P1 and S1P5) were not found to enhance remyelination after cuprizone diet, but do prevent demyelination when administered simultaneously with cuprizone.[15–19] In 2021, the S1P1 mono-selective modulator ponesimod was marketed for RRMS (Ponvory, Janssen©). Ponesimod shows high selectivity for S1P1, and the OPTIMUM trial indicated that ponesimod treatment reduced annual relapses and fatigue symptoms.[20] As S1P1 expression is higher in immature OPCs compared to the other S1PR subtypes, the mono-selectivity of ponesimod is an interesting characteristic for studying OPC differentiation and myelination.[14] A previous study indicated that ponesimod increases myelination in the cingulum in the cuprizone mouse model of demyelination.[21] In this study, we studied the potential of ponesimod to enhance remyelination and to improve remyelination-associated functions in the cuprizone model of demyelination and to enhance primary mouse OPC differentiation.

2 | MATERIALS AND METHODS

2.1 | Animals

For the cuprizone experiment, 8-week-old C57Bl6OlaHsd mice were purchased from Envigo (Horst, The Netherlands). Animals were co-housed during the first week of acclimatization. Next, mice were housed individually until the end of the experiment. All animals had ad libitum access to food and water and were kept in a humidity and temperature-controlled room under a 12-h light/dark cycle (lights on at 6 AM and lights off at 6 PM). Experiments were conducted in accordance with institutional guidelines of the ethical committee for animal experiments of Hasselt University (Ethical matrix ID 202152).

2.2 | Cuprizone and treatment

To induce demyelination, 8-week-old male C57BL/6JOlaHsd mice were fed 0.3% cuprizone (Sigma-Aldrich, Belgium) in normal chow (Sniff, Germany) or a normal chow placebo diet (Sniff, Germany) for a total of 6 weeks. Cuprizone chow was provided ad libitum. After the 6-week demyelination phase, the cuprizone diet was terminated, and mice

received a normal chow diet, initiating the remyelination phase. Three days prior to ending the cuprizone diet, oral treatment with ponesimod was started and maintained for 10 days. Oral gavage with an injection volume of 10 μL/g was performed once daily. Mice received either vehicle (0.5% methylcellulose, 2% Tween80, 0.5% DMSO), ponesimod (1, 3, or 10 mg/kg) (Janssen, Beerse, Belgium), or clemastine fumarate 10 mg/kg (Ambinter, France) as a positive comparative control. All groups were balanced for baseline results of VEP and Y maze (Figure S1). A group of $n = 11$ of cuprizone-fed mice was sacrificed on the day the cuprizone diet ended, as described below. Weights were monitored regularly from the start of cuprizone diet.

2.3 | Spatial alternation Y maze

All mice were subjected to the spatial alternation Y maze at the end of the demyelination phase (during the final week of cuprizone diet, on days 35 and 36 of diet) and during the remyelination phase (during treatment week after stop of cuprizone, on days 6 and 7 of treatment). The Y maze has three similar 40-cm-long arms that are all placed 120° from each other. Each arm contained a visual cue. During this one-trial test, the mice were placed into the maze facing the center and were able to freely explore the maze for 2 min. Arm entries were manually registered and considered valid when both hind paws were entirely inside the arm. A consecutive visit to three different arms defines a correct triad. The measure for working memory is calculated as the percentage of correct alternations (alt% = number of triads/(number of arm entries − 2)*100). Animals not exploring at least three triads over the 2-min trial were excluded. The Y maze was always performed in the dark phase of the day/night cycle.

2.4 | Visual evoked potentials (VEPs)

All mice were subjected to VEP measurements at the end of demyelination (during the final week of the cuprizone diet, on days 37 and 38 of diet) and during remyelination (during treatment week after stop of cuprizone, on days 8 and 9 of treatment).[22] In brief, animals were dark-adapted for at least 3 h prior to the start of VEP to increase light sensitivity. Animals were anesthetized by intraperitoneal (i.p.) injection with xylazine (20 mg/kg) and ketamine (80 mg/kg). Pupils were dilated using 1% tropicamide for 5 min, and subsequently with 2.5% phenylephrine hydrochloride for 1 min. Next, an active electrode was placed subdermally at the visual cortex, a ground electrode was inserted at the base of the tail to prevent electromagnetic noise from the environment, and finally, a reference electrode was inserted in the tongue (CELERIS system, Diagnosys). Lastly, the eyes were moistened with saline and the flash electrodes were placed on the eyes. Impedance measurement was used to evaluate electrode connection before starting the VEP. Mice were presented with 200 white light flashes, each with a duration of 310 ms. The stimulus frequency was set at 1 Hz and stimulus intensity was set at 0.5 cd s/m^2. Latency time (i.e., time between visual flash stimulus and the arrival of the signal in the visual cortex) was given in milliseconds (ms), being reflective of the myelination status of the visual tract (Diagnosys ESPION software). All VEP experiments were completed in the dark.

2.5 | Sacrifice and tissue collection

Animals were sacrificed by means of pentobarbital overdose (Dolethal, 200 mg/kg), followed by transcardial perfusion with PBS/heparin. Two hours prior to sacrifice, mice received a final oral treatment with vehicle, clemastine fumarate, or ponesimod. Brains were dissected and the corpus callosum was dissected from the rostral part and brought into 2% glutaraldehyde fixative for transmission electron microscopy (TEM) analysis. The caudal part was entirely fixated in 4% paraformaldehyde for 24 h and subsequently brought in a sucrose gradient (10% > 20% > 30%) for cryoprotection. Coronal sections of 5 μm were sectioned on a cryostat (Leica).

2.6 | MBP immunohistochemistry

Cryosections were fixated in ice-cold acetone for 10 min and air-dried for 30 min. Sections were incubated in blocking buffer (0.05% Triton X100 + 10% DAKO protein block in PBS) for 20 min. Next, sections were incubated with rat anti-MBP (Millipore, MAB386, 1/500) diluted in blocking buffer overnight at 4°C. Samples were incubated with anti-rat Alexa 555 secondary antibody (Life technologies, A21434, 1/400) diluted in PBS for 1 h. Nuclei were counterstained with DAPI and slides were mounted using Fluoromount G (Invitrogen). Samples were imaged using the Leica DM2000 LED fluorescence microscope. Quantification was performed in FIJI ImageJ based on the MBP+ area percentage.

2.7 | Transmission electron microscopy

Following fixation, post-fixation was performed with 2% osmium tetroxide in 0.05 M sodium cacodylate buffer (pH = 7.3) for 1 h at 4°C. Dehydration of the samples was

performed by ascending concentrations of acetone. The dehydrated samples were impregnated overnight in a 1:1 mixture of acetone and araldite epoxy resin. Afterward, the samples were embedded in Araldite epoxy resin at 60°C and were cut into slices of 70 nm with a Leica EM UC6 microtome. Slices were transferred to 0.7% formvar-coated copper grids (Aurion) and the tissue was cut perpendicular to the corpus callosum. Images were obtained with a Jeol JEM-1400 Flash transmission electron microscope equipped with an Emsis 20 MP XAROSA CMOS camera. Analysis of G-ratio (= diameter axon only/diameter axon with myelin sheath) was performed in ImageJ.

2.8 | Primary mouse OPC differentiation assay

Primary mouse OPCs were isolated from C57BL/6JOlaHSD pups on postnatal day 0 or 1 using the shake-off method as described before.[23] OPCs were plated in differentiation medium (DMEM high-glucose with 2% horse serum, 2% B-27, 50 U/mL pen/strep, 0.3 mM transferrin, 0.5 mM L-thyroxine, 0.1 mM putrescin, 0.02 mM progesterone, 0.5 μM tri-iodo-thyronine, 0.2 μM sodium selenite, and 0.8 mM insulin, all from Sigma-Aldrich) at a density of 250.000 cells onto poly-L-lysine coated glass coverslips in 24-well tissue culture plates. One hour after plating, the cells were allowed to proliferate by adding platelet-derived growth factor (PDGF; 10 ng/mL; Peprotech) and fibroblast growth factor (FGF; 10 ng/mL; Peprotech) for 24 h, followed by 24-h treatment with FGF only. Next, FGF-containing medium was removed and cells were treated with ponesimod (Janssen, Beerse, Belgium), ozanimod (MedChem), A971432 (Tocris), fingolimod-phosphate (P-FTY720, Cayman Chemical), or siponimod (MedChem) in 0.1% DMSO (Sigma). Compounds were used in a concentration of 300 nM, 1 μM, and 3 μM. Every 48 h, treatment was repeated with a 50% medium change up until 6 days of compound treatment. Cells were fixated in 4% paraformaldehyde and non-specific binding was blocked for 30 min with 1% bovine serum albumin (BSA; Sigma) in 0.1% PBS-T, followed by incubation with a mouse anti-O4 (R&D systems, MAB1326, 1/1000) and a rat anti-MBP (Millipore, MAB386, 1/500) primary antibody overnight at 4°C. After washing, a goat anti-mouse Alexa 488-conjugated (Life Technologies, A21042, 1/600) or goat anti-rat Alexa 555-conjugated (Life Technologies, A21434, 1/600) secondary antibody was added for 1 h. Coverslips were incubated with a DAPI nuclear stain for 10 min, mounted with fluoromount G mounting medium (Invitrogen), and imaged at 20× magnification using a fluorescence microscope (Leica DM2000 LED). Five random images per coverslip were taken and a readout of MBP+ area and O4+ area corrected for DAPI+ area (within well) was obtained using Fiji ImageJ software. Values were normalized to vehicle condition. A dose-finding experiment for the O4 and MBP ICC was performed prior to the differentiation experiment (Figure S2).

2.9 | Primary mouse OPC fiber myelination assay

After shake-off, OPCs were plated at a density of 50.000 cells per poly-L-lysine coated fiber scaffold (Amsbio, AMS. TECL-006-1X).[24] One hour after plating, the cells were treated with compound or vehicle identical to the differentiation assay. Every 48 h, treatment was repeated with a 50% medium change. On day 14, the cells were fixated in 4% paraformaldehyde and permeabilized with 0.1% PBS-T for 10 min. Next, cells were incubated overnight at 4°C with a rat anti-MBP (Millipore, MAB386, 1/200) primary antibody in PBS. Cells were incubated with goat anti-rat Alexa 488-conjugated (Invitrogen, A11006, 1/1000) secondary antibody for 1 h in PBS. Nuclei were counterstained with DAPI and the fibers were mounted onto glass microscope slides with fluoromount G mounting medium (Invitrogen) and imaged with a 40× water/NA0.55 objective using a Zeiss LSM880 confocal airyscan microscope. Confocal stacks of 0.5 μm z-steps were taken. Per scaffold, six random cells were completely imaged and bidirectional MBP+ sheath length per cell was quantified in blinded confocal images using FIJI ImageJ software. Before confocal imaging of MBP, the Olig2 signal was checked on a regular fluorescence microscope (Leica DM2000 LED).

2.10 | Primary mouse OPC migration assay

OPCs were seeded in an agarose drop at a density of 100.000 cells per drop after shake-off.[25] Briefly, 21 μL of 1% agarose was added to 42 μL of cell suspension that contained 5×10^6 cells in total. Drops of 1.5 μL were made in a 24-well tissue culture plate. After setting for 15 min at 4°C, 50 μL of differentiation medium was added around the drop, and plates were incubated for 2 h at 37°C and 8.5% CO_2. Next, 450 μL of compound-containing differentiation medium was added to the cells to obtain a final concentration of 3 μM compound and 0.1% DMSO. Agarose drops were imaged in the IncuCyte (Sartorius, Göttingen, Germany), where images were taken through a 4× objective at day 0 and day 5. Cells that migrated from the agarose drop were manually quantified using FIJI ImageJ software with respect to the image taken at timepoint zero.

2.11 | Quantitative PCR

OPCs were plated at 250.000 cells per glass coverslip in 24-well plates. Twenty-four hours after PDGF and FGF treatment, cells were treated with ponesimod in concentrations ranging from 0.3 to 3000 nM or 0.1% DMSO on days 1 and 3 and lysed on day 4. Total RNA was isolated from primary OPCs, using the RNeasy mini kit (Qiagen), according to the manufacturer's instructions. RNA concentration and quality were analyzed with a Nanodrop spectrophotometer (Isogen Life Science). RNA was reverse-transcribed using the qScript cDNA Supermix kit (Quanta). qPCR was performed using the Applied Biosystems QuantStudio 3 Real-Time PCR System (Life Technologies). The reaction mixture consists of SYBR Green master mix (Life Technologies), 10 μM forward and reverse primers (Table S1), nuclease-free water, and cDNA template (12.5 ng), up to a total reaction volume of 10 μL. Results are analyzed by the comparative Ct method and normalized to the most stable housekeeping genes (β-actin, Ywhaz), determined by GeNorm.

2.12 | Statistical analysis

All data were statistically analyzed using GraphPad 9.2.0. software (GraphPad Software Inc., CA, USA). Data are expressed as mean values ± standard error of the mean (SEM). Outliers were calculated based on Dixon's *Q*-test and were excluded from the dataset (α .05). Normality was checked using the Shapiro–Wilk test. For de- and remyelination Y maze data analysis, a one-sample *t*-test was performed against a 50% chance level. For VEP data in the demyelination phase, the cuprizone group and the no cuprizone group were compared in a Mann–Whitney test. VEP remyelination data, MBP IHC data, and TEM data analysis were performed by means of one-way ANOVA followed by Dunnett's multiple comparisons test, or Kruskal–Wallis followed by Dunn's multiple comparisons test according to data normality. The multiple comparisons included three doses of ponesimod compared to vehicle. The clemastine-treated group, the untreated cuprizone group, and the no cuprizone group serve as a validation of the used model and are thus not included in the statistical comparisons. In VEP, MBP IHC, and TEM analysis, the clemastine-treated positive control was compared to vehicle alone in an unpaired *t*-test, as performed in the sample size calculations for these experiments (G*power). For in vitro OPC experiments, data were normalized against a within plate 0.1% DMSO vehicle control group. For all testing conditions, a one-sample *t*-test was performed against a control value of 1. Alpha was manually corrected for multiple comparisons. *p*-Values are indicated in the figure descriptions. $*p < .05$, $**p < .01$, $***p < .001$.

3 | RESULTS

3.1 | Ponesimod reverses cuprizone-induced memory impairment and decreases latency time of the optic nervous system

First, we investigated whether ponesimod could improve working memory impairment featuring the cuprizone model. During the final week of the cuprizone diet, being the demyelination phase, only the "no cuprizone" animals receiving a control diet showed intact working memory (73.61 ± 6.9%; *p* .0192) whereas the cuprizone-treated mice displayed impaired working memory (55.77 ± 5.6%, *p* .3191) (Figure 1A), confirming the validity of the test. When working memory was assessed during the remyelination phase, mice previously on the cuprizone diet treated with ponesimod 1 mg/kg (80.05 ± 2.6%, *p* .0003) and ponesimod 3 mg/kg (60.68 ± 4.2%, *p* .0280) displayed restored working memory, whereas the vehicle-treated mice did not show an improved working memory (Figure 1B). In parallel, we assessed whether ponesimod could reduce the latency time of VEPs in the cuprizone model. During the final week of the demyelination phase, the cuprizone-fed animals showed an increase in latency time (59.47 ± 0.80 ms, *p* .0059) compared to the "no cuprizone" animals (53.16 ± 2.83 ms, *p* .0059), reflective of demyelination (Figure 1C). When VEPs were assessed during the remyelination phase, mice treated with ponesimod 1 mg/kg (54.53 ± 1.99 ms, *p* .0034) and ponesimod 10 mg/kg (55.98 ± 1.58 ms, *p* .011) showed a reduction in latency time compared to the vehicle-treated mice (64.06 ± 1.12 ms) (Figure 1D). The positive control group was treated with clemastine fumarate (10 mg/kg) and showed a decrease in latency time when compared to vehicle in an unpaired *t*-test (53.80 ± 2.307 ms, *p* .0015). These data support a restoration of the working memory and VEPs during the remyelination phase by ponesimod in a dose of 1 mg/kg. All in vivo experiments were conducted according to the timeline represented in Figure 1E.

3.2 | Ponesimod enhances remyelination in the corpus callosum, cortex, and hippocampus

To determine remyelination levels, we quantified the area of myelin basic protein (MBP) in the medial corpus callosum, the cortex dorsal to the corpus callosum,

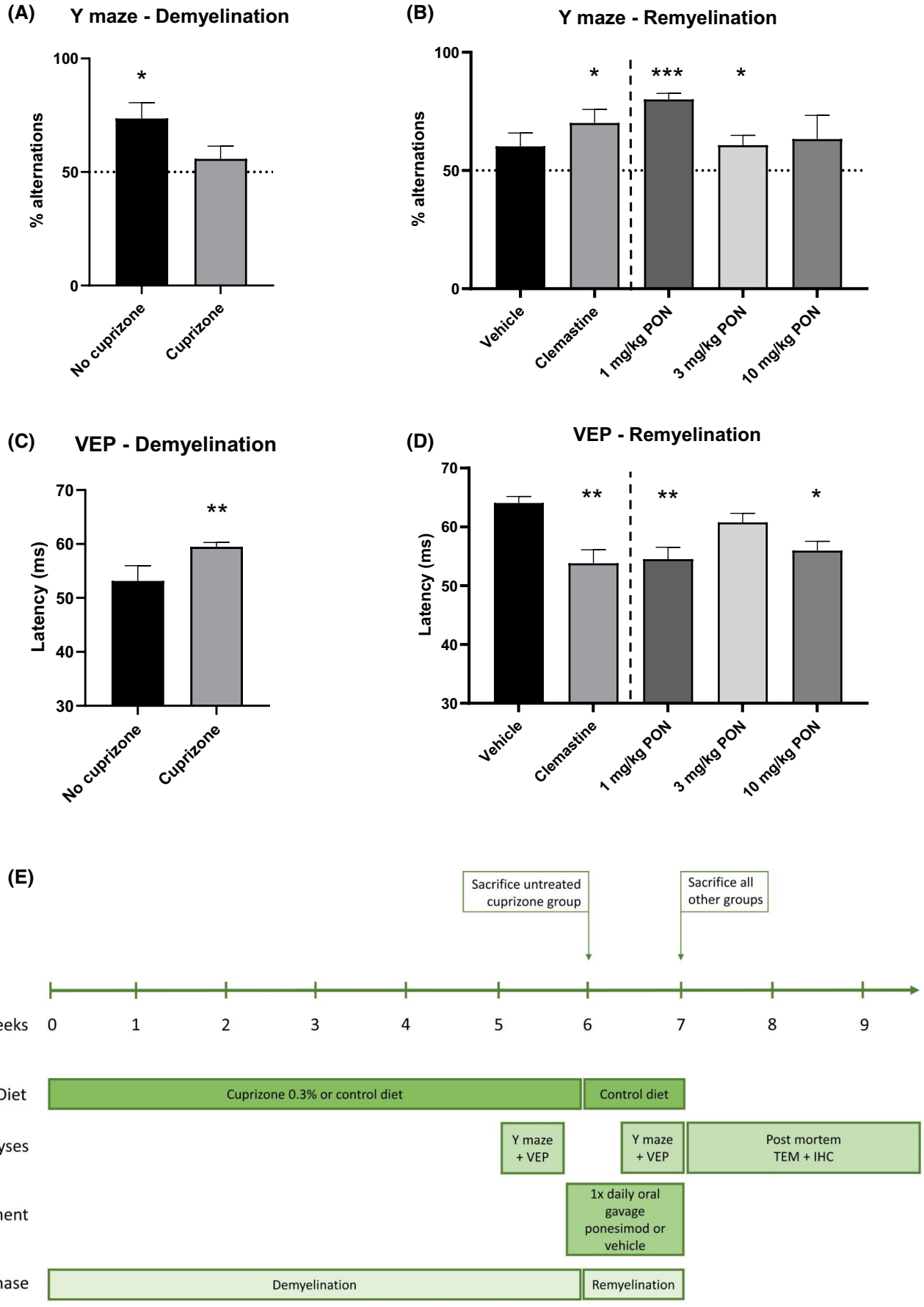

FIGURE 1 Working memory performance assessed by the Y-maze and assessment of visual evoked potentials during demyelination and remyelination. In the Y maze, the percentage of alternations (A, B) is calculated based on the number of correct triads during a 2-min trial. Data are compared to the hypothetical chance level of 50% using one-sample *t*-test. Latency time from VEPs (C, D) is given as a measure for fiber myelination. Demyelination data were compared using a Mann–Whitney test. VEP remyelination data were analyzed by means of a Kruskal–Wallis test with Dunn's multiple comparisons including three doses of ponesimod compared to vehicle. $n = 9$-10 animals per condition. The clemastine-treated group was compared to vehicle in an unpaired *t*-test. A timeline on the performance of all in vivo experiments is shown (E). Data are presented as mean ± SEM. $*p < .05$, $**p < .01$, $***p < .001$.

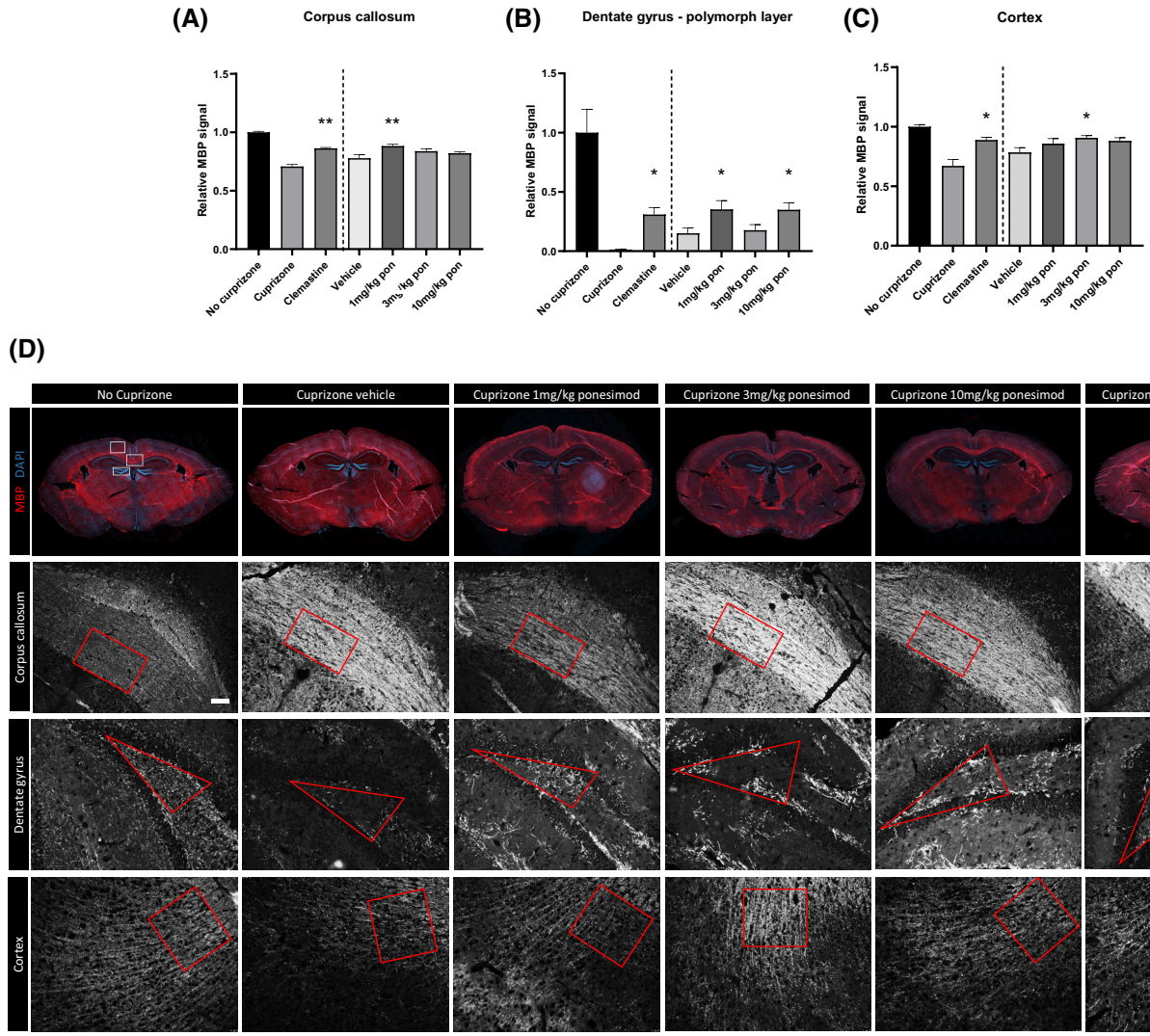

FIGURE 2 MBP fluorescent staining of the corpus callosum (A), the dentate gyrus of the hippocampus (B), and the cortex (C) at the remyelination phase. Representative images were shown (D). MBP+ area percentage was determined using the Fiji ImageJ software. Data were analyzed by means of one-way ANOVA with Dunnett's multiple comparisons (corpus callosum and hippocampus) or Kruskal–Wallis test with Dunn's multiple comparisons (cortex) including three doses of ponesimod compared to vehicle. $n = 9$-10 per condition. The clemastine-treated group, the untreated cuprizone group, and the no cuprizone group were compared to vehicle in an unpaired *t*-test. The red outlines indicate the analyzed area. Scale bar is 50 μm. Data are presented as mean ± SEM. $*p < .05$, $**p < .01$.

and the dentate gyrus of the hippocampus in coronal slices (bregma AP −1.50 mm). An ANOVA analysis and Dunnett's multiple comparisons on the MBP quantification in the medial corpus callosum (Figure 2A) revealed increased myelination following ponesimod 1 mg/kg (0.8827 ± 0.015, *p* .0031) treatment. Analysis of the dentate gyrus of the hippocampus (Figure 2A) showed an increase in myelination after ponesimod 1 mg/kg (0.3524 ± 0.074, *p* .0445) and ponesimod 10 mg/kg (0.3497 ± 0.057, *p* .0412) treatment. MBP quantification in the cortex (Figure 2C) revealed increased myelination by ponesimod 3 mg/kg only in the Kruskal–Wallis

test with Dunn's multiple comparisons (0.9067 ± 0.018, p .0232). Additionally, TEM analysis of the corpus callosum revealed a decrease in G-ratio for treatment with ponesimod 1 mg/kg (0.7887 ± 0.009, p .0282), 3 mg/kg (0.7911 ± 0.010, p .0375), and 10 mg/kg treatment (0.7655 ± 0.007, p .0002) (Figure 3).

3.3 | Ponesimod improves OPC differentiation without altering myelination capacity or cell migration in vitro

To investigate the remyelination-promoting potential of selective S1P1 modulation, we evaluated the effect of ponesimod on OPC differentiation compared to others in class. Dose determination was performed by means of qPCR for immature OPC and mature oligodendrocyte markers. We found a trend toward increased expression of multiple oligodendrocyte maturation genes upon treatment with concentrations between 100 and 3000 nM (Figure 4A). Moreover, qPCR analysis revealed that upon ponesimod treatment, mRNA expression of S1P1 is not altered (Figure 4B). The effect of A971432 (mono-selective S1P5), ozanimod (dual S1P1 and S1P5), siponimod (dual S1P1 and S1P5), a combination of ponesimod and A971432, and P-FTY720 (non-selective) on primary mouse OPC differentiation was evaluated by analyzing O4+ area (pre-mature oligodendrocyte marker) and MBP+ area (late differentiated oligodendrocyte marker). Fluorescent ICC shows increased O4 expression in primary OPCs upon treatment with ponesimod alone (300 nM; p .0028 and 3000 nM; p .0027) and upon combination treatment with ponesimod and A97 1432 (300 nM; p .0002 and 1000 nM; p .0015) after 6 days (Figure 4C). Although trends were observed, we did not detect a significant increase in MBP expression in

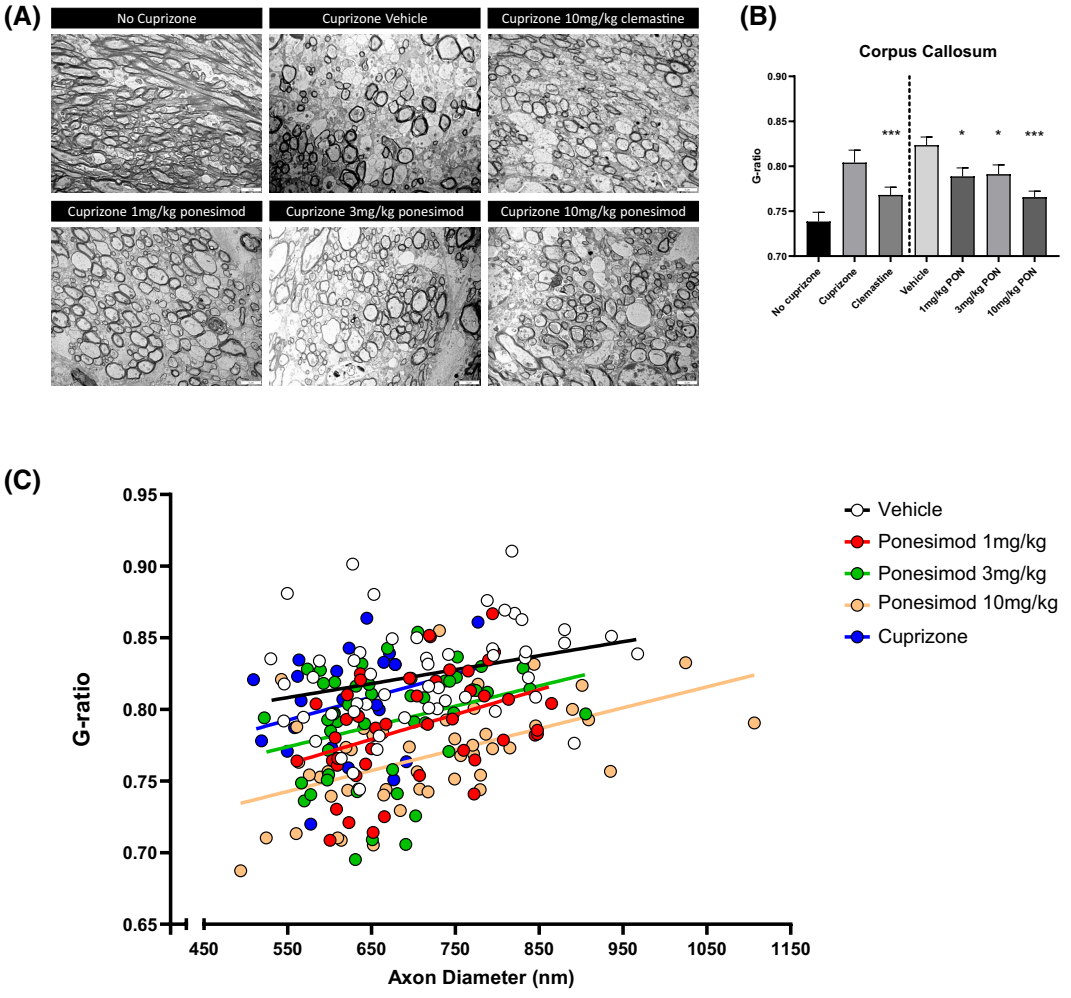

FIGURE 3 TEM of the corpus callosum at the remyelination phase (A). G-ratios were calculated using the Fiji ImageJ software (B, C). Data were analyzed by means of one-way ANOVA with Dunnett's multiple comparisons. n = 9-10 per condition. The clemastine-treated group, the untreated cuprizone group, and the no cuprizone group were compared to vehicle in an unpaired t-test. Scale bar is 2 µm. Data are presented as mean ± SEM. *p < .05, **p < .01, ***p < .001.

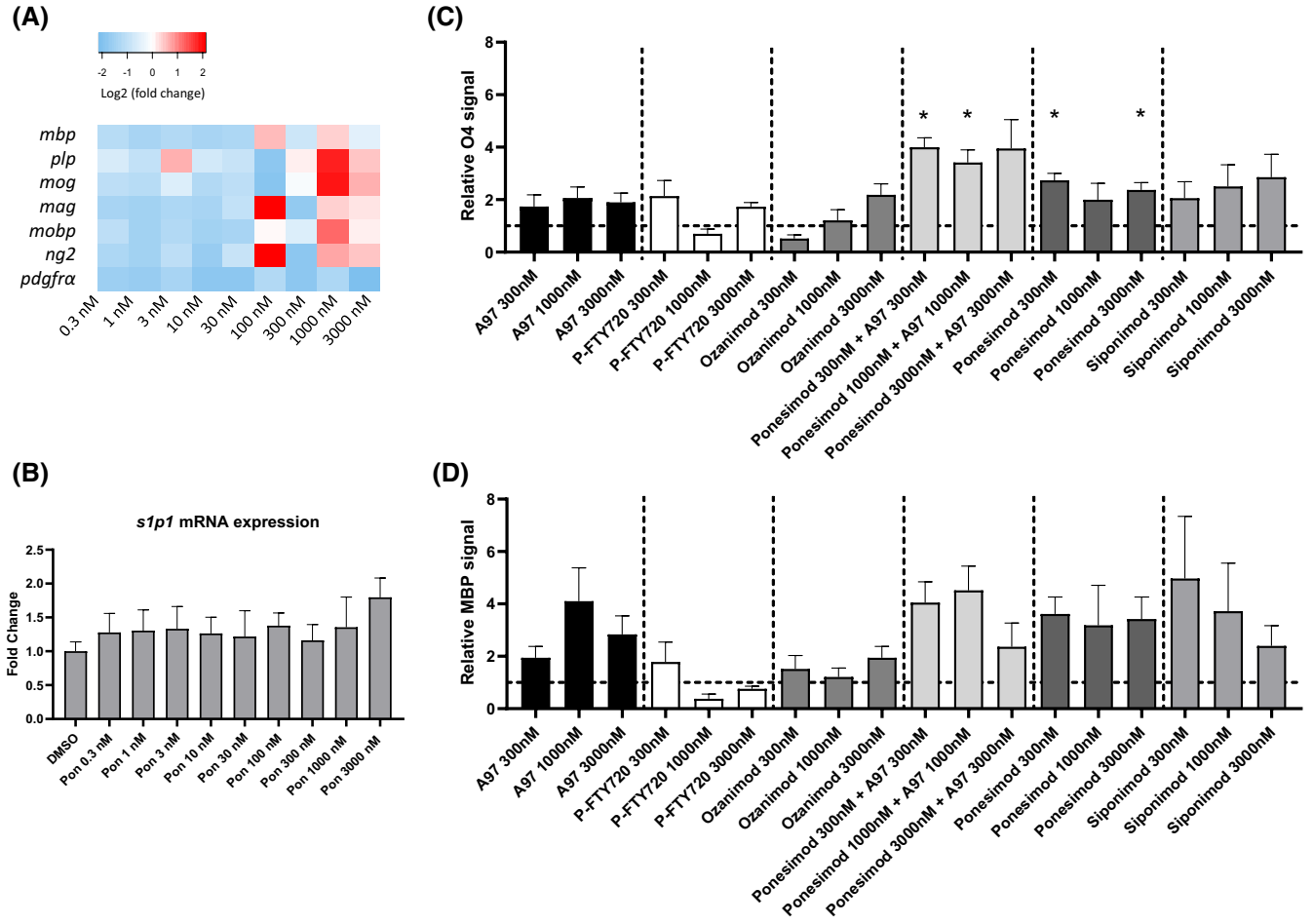

FIGURE 4 Ponesimod increased differentiation of primary mouse OPCs. The expression of mature oligodendrocyte genes in primary mouse OPCs increased upon treatment with 100–3000 nM ponesimod (A). Expression of the S1P1 gene in OPCs treated with ponesimod is not altered (B). Immunocytochemical staining for oligodendrocyte marker O4 (C) revealed enhanced O4 expression in response to ponesimod (300 and 3000 nM) and dual ponesimod + A971432 (300 and 1000 nM) treatment on day 6. Immunocytochemical staining for MBP (D) did not reveal significant differences in MPB expression between conditions. Representative microscope images (E) of primary OPCs treated with the respective compounds on day 6. A one-sample *t*-test was performed against a control value of 1 (DMSO 0.1%). Alpha was corrected for multiple comparisons ($\alpha = .0028$). Scale bar is 50 μm. Data are represented as mean ± SEM. *$p \leq .0028$. *mbp*, myelin basic protein; *plp*, myelin proteolytic protein; *mog*, myelin oligodendrocyte glycoprotein; *mag*, myelin-associated glycoprotein; *mobp*, myelin-associated oligodendrocyte basic protein; *pdgfrα*, platelet-derived growth factor receptor *α*; *ng2*, neuron glial 2.

primary OPCs upon treatment with any of the compounds after correction for multiple comparisons (Figure 4D).

In the in vitro fiber myelination assay, fluorescent ICC for MBP does not show increases in MBP-positive sheath length upon treatment with any of the compounds tested (Figure 5A). Moreover, treatment with A971432 (300 nM), P-FTY720 (300 and 1000 nM), and ozanimod (300 nM) decreased MBP-positive sheath length. When assessing the outcome of ponesimod 3 μM on the extent of primary mouse OPC migration, we observed no alterations in migration distance after 5 days (Figure 5C). A significant decrease in migration distance was observed in P-FTY720 3 μM treated cells (p .0011). The other compounds tested did not alter OPC migration.

4 | DISCUSSION

This manuscript describes the effect of ponesimod, a selective S1P1 functional antagonist, on functional outcome and remyelination in the cuprizone model and on OPC differentiation in vitro. We found the cuprizone-induced working memory impairment to be reversed upon treatment with ponesimod 1 and 3 mg/kg. Moreover, we found VEPs to show reduced latency time upon 1 and 10 mg/kg ponesimod treatment. When assessing remyelination in the cuprizone model, ponesimod-treated groups show increased MBP area and decreased G-ratio in the corpus callosum. Finally, results show that ponesimod increases OPC differentiation into mature oligodendrocytes, but does not affect in vitro fiber wrapping.

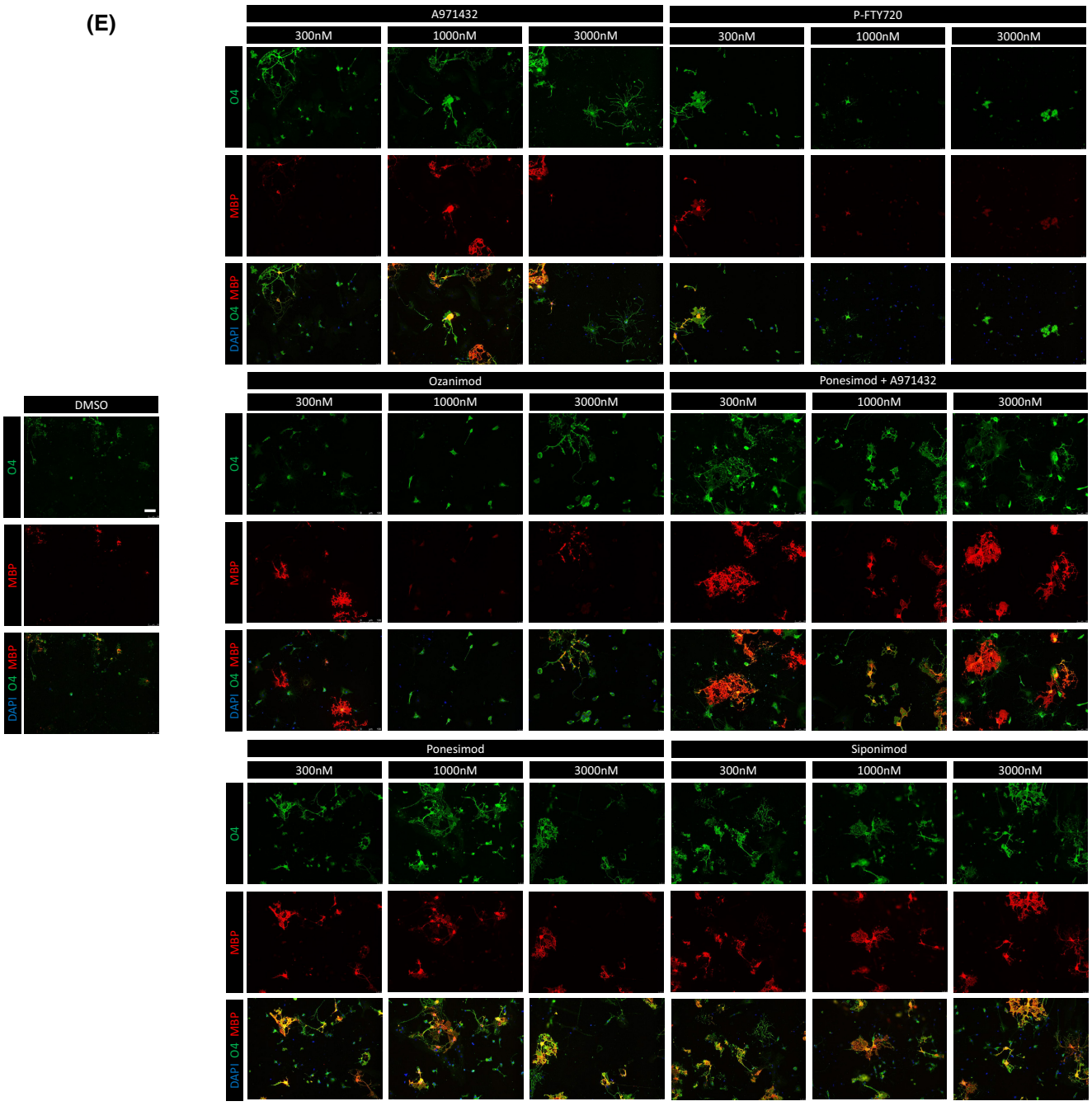

FIGURE 4 (Continued)

The remyelination-promoting characteristic of ponesimod could be mediated by stimulating OPC differentiation, likely through interaction with other cell types, for example, astrocytes.[21] Within the used cuprizone model, and dependent on the evaluated brain area, there is no clear dose-response effect.

FIGURE 5 Immunocytochemistry fiber MBP staining and OPC migration assay. Immunocytochemical staining for MBP (A) did not show an effect of ponesimod on MBP sheath length in primary mouse OPCs in the fiber myelination assay. Treatment with A971432 (300 nM), P-FTY720 (300 and 1000 nM), and ozanimod (300 nM) decreased MBP-positive sheath length. Representative MBP confocal stacked images (B) of primary OPCs on the fiber scaffolds treated with the respective compounds on day 14. We report that upon P-FTY720 3-μM treatment, OPC migration is significantly decreased (C). Cells that migrated from the agarose drop were manually quantified (D). Alpha was corrected for multiple comparisons ($\alpha = .0028$). A one-sample *t*-test was performed against a control value of 1 (DMSO 0.1%). Scale bar is 10 μm. Data are represented as mean ± SEM. *$p \leq .0028$.

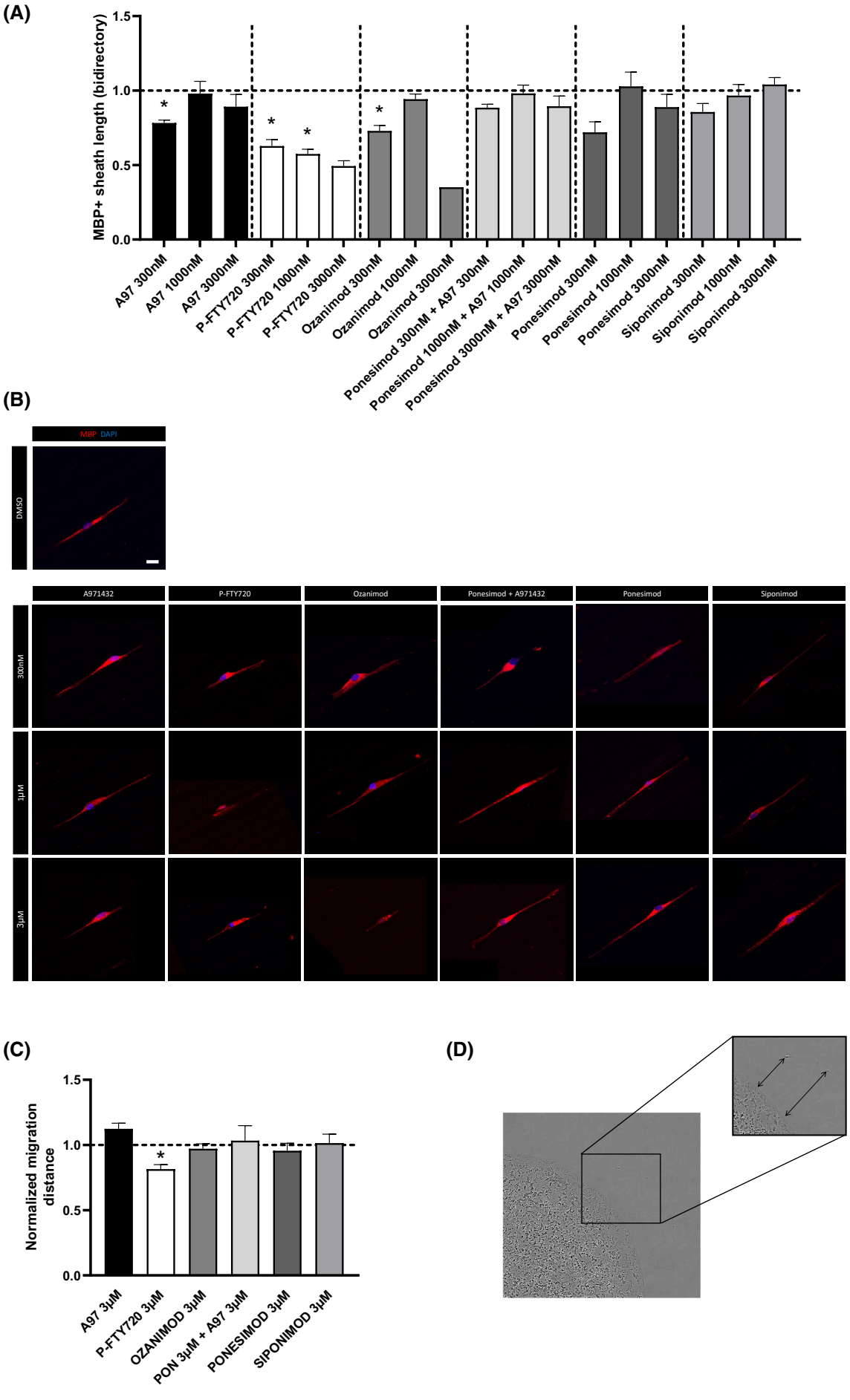

This is the first time the effect of S1PR modulation was assessed on cuprizone-induced working memory deficits and VEPs in rodents. Previously, siponimod and ozanimod, both dual S1P1 and S1P5 modulators, have shown clinically meaningful benefits on cognitive function in patients with SPMS and RRMS, respectively (EXPAND and SUNBEAM trials).[26,27] Moreover, FTY720 and ozanimod were shown to improve memory function in a cisplatin-fed mouse model.[28] Selective S1P1 modulation by ponesimod has not been evaluated for cognitive performance before, neither in rodents nor in a human trial. Additionally, we included VEPs as a highly translational non-invasive functional test that provides a measure of axonal de-/remyelination. In humans, VEP provides paraclinical data in terms of MS diagnosis and therapeutic monitoring.[29] Although rodent visual pathways differ in complexity from those of humans, VEP implements direct information on the optic nerve and related cortex functionality, providing a non-invasive translational measure for myelination in the cuprizone mouse model.[30,31] After 6 weeks, cuprizone-fed mice show an increased latency of the VEPs, reflective of demyelination in the optic trajectory. After treatment with ponesimod 3 and 10 mg/kg, we found latency times to be restored, indicative of remyelination.

The ponesimod-induced effect in memory-related processes and increase in the signaling speed of the visual pathway might be due to an increase in myelination. We showed that ponesimod increased MBP+ area in the corpus callosum, hippocampus, and cortex in cuprizone-fed mice. Moreover, TEM analysis of the corpus callosum showed that ponesimod decreased G-ratio, reflective of remyelination. In line with our findings, it was recently reported that in a paradigm of 6 weeks of 0.2% cuprizone, followed by 3 weeks of oral administration of ponesimod 30 mg/kg twice daily improved remyelination in the cingulum, a limbic structure dorsal to the corpus callosum related to MS fatigue.[21] Interestingly, in this study, myelination in the corpus callosum was not affected.[21] Moreover, when applying a 1-week treatment in the same cuprizone paradigm, myelination in the corpus callosum was even further decreased.[21] In contrast, our results reveal that 1 week of 1 mg/kg ponesimod treatment once daily after 6 weeks of 0.3% cuprizone diet restored myelination in the corpus callosum as assessed with TEM and MBP staining. These different findings concerning the remyelination in the corpus callosum can be attributed to the applied cuprizone concentration, the dose of ponesimod during treatment phase, or the duration of the treatment. In our study, a cuprizone concentration of 0.3% was applied as this paradigm has shown the preferable characteristics to study the direct effect of ponesimod in the remyelination window after cuprizone stop. More specifically, the demyelination process in the corpus callosum reaches its peak after 6 weeks of diet, without the occurrence of endogenous remyelination.[32] Furthermore, the applied doses within the current study were based on the human dose of ponesimod (Ponvory, J&J) of 20 mg once daily. After performing human equivalent dose calculations as recommended by the US Food and Drug Administration, the murine dose results in 4.1 mg/kg, finally resulting in a dose range of 1, 3, and 10 mg/kg ponesimod.[33] Finally, the single daily dose in our therapeutic paradigm is suggested to be sufficient, based on the relatively long half-life of ponesimod in humans, being between 21.7 and 33.4 h with doses ranging from 1 to 75 mg.[34] Nonetheless, studying cuprizone-induced demyelination in male C57BL/6J mice only may have limitations due to sex-dependent differences in prevalence and severity of MS.

Whether the ponesimod-induced increase in myelination is directly mediated by improved functioning of oligodendrocytes remained unknown. It has previously been published that functional antagonism by ponesimod increases viability in a cuprizone-treated oligodendrocyte cell line.[35] In contrast, other research showed that S1P1-deletion leads to a delay in OPC differentiation during early myelination in mice (3 weeks old), but does not show a phenotypic effect in adult life (3 months old).[36] Therefore, it is debatable whether a takeover of compensatory mechanisms occurs during development. We evaluated the direct effect of ponesimod on primary mouse OPC differentiation, migration, and myelination in vitro in a high-purity OPC culture. S1PR modulators siponimod (dual S1P1 and S1P5), ozanimod (dual S1P1 and S1P5), P-FTY720 (S1P1, S1P3, S1P4, and S1P5), and A971432 (S1P5 selective) were included in the in vitro experiments to compare the effect of modulator selectivity. We found that ponesimod enhances mouse OPC differentiation based on O4 immunocytochemistry, a marker for early oligodendrocyte differentiation.[37] Upon combination treatment with A971432, a selective S1P5 modulator, the observed effect was even enhanced. In an initial dose-finding experiment, we found concentrations of 100-3000 nM ponesimod to show a trend toward increased expression of oligodendrocyte maturation genes (*plp, mog, mag, mobp, mbp*), while *pdgfrα* gene expression showed a decreasing trend. An intermediate concentration of 300 nM did not show a similar effect, possibly partly due to the high variability in primary OPC cultures, and the low RNA yield from these cultures. Interestingly, a trend toward enhanced *ng2* expression, being reflective of an immature OPC population, was observed upon ponesimod treatment. However, literature suggests NG2+ cells express two distinct markers of early oligodendrocytes, specifically PDGFRα and O4. During early differentiation, PDGFRα expression typically decreases while O4 expression increases, supporting that NG2+ cells are dedicated to the oligodendrocyte lineage.[38–40]

S1P1 is a Giα-coupled receptor which upon activation stimulates ERK and Akt signaling while inhibiting adenylate cyclase, the enzyme that produces cyclic adenosine monophosphate (cAMP).[41] Functional antagonism of S1P1 by ponesimod is expected to decrease Giα activity and, therefore, to increase cAMP production, which is beneficial for OPC differentiation.[22,42–44] Moreover, S1P1 functional antagonism results in reduced MAPK-ERK signaling. It was previously reported that inhibition of ERK signaling increases differentiation of neural progenitor cell-derived OPCs, supporting the effect of S1P1 functional antagonism on OPC differentiation.[45] In this study, we show that ponesimod treatment in OPCs does not increase S1P1 mRNA levels, indicating that sustained pharmacological S1P1 internalization does not increase expression of S1P1 as a compensatory mechanism.[21] S1P5 functional antagonism by the mono-selective A971432 does not have an effect on OPC differentiation. It was previously shown that S1P5 deficient mice do not show any myelination deficits.[46,47] Therefore, S1P5 is likely not necessary for the induction of myelination. Moreover, S1P5 is lowly expressed in immature OPCs compared to S1P1. Dual S1P1 and S1P5 modulation by siponimod showed a trend toward increased OPC differentiation, while ozanimod did not. Previous research elucidated a species-based difference of S1P5 selectivity of ozanimod, which shows reduced potency for mouse S1P5 resulting from a mutation of threonine to alanine at position 120.[19] Nonetheless, it was shown that mice are up to 11-fold less efficient in generating the major ozanimod metabolite (CC112273).[48] Therefore, ozanimod might require human metabolization for full receptor engagement.[49,50]

In our study, we confirm that functional antagonism of S1P1 by ponesimod drives OPC differentiation, a key step in initiating (re)myelination, but does not affect axonal wrapping by OPCs in vitro. We can deduce that an individual OPC-oligodendrocyte will not perform more axon wrapping upon ponesimod treatment. The ponesimod-induced increase in myelination in the cuprizone model could be attributed to an increase of maturating myelinating cells in the tissue. Moreover, it has been shown that ponesimod blocks astrocytic neuroinflammatory responses and increases the number of GFAP+ cells in the corpus callosum of cuprizone-fed mice. The astrocyte–oligodendrocyte interplay possibly contributes to increased wrapping in vivo.[21]

Due to the non-selective S1PR modulator P-FTY720 significantly inhibiting OPC migration, it was hypothesized that modulating both S1P1 and S1P5 is responsible for the decrease in cell migration. However, this study shows that dual modulation, both by the combination of ponesimod and A971432, as well as the dual modulators ozanimod and siponimod, did not affect OPC migration. The expression of S1P5 gradually increases during maturation of OPCs toward mature myelinating oligodendrocytes. S1P5 can couple two types of G-proteins: Giα and/or G12/13. Which G-protein is coupled depends on the maturation stage of the oligodendroglial cell.[14] Early in maturation, activation of the G12/13 protein induces Rho/ROCK signaling, which causes process retraction and inhibits cell migration. Later in maturation, the Giα protein activates ERK/Akt signaling upon S1P5 activation.[46,47] Activation of S1P5 by the natural S1P ligand blocks OPC migration in a transwell migration assay.[51] This S1P-induced change in OPC migration was prevented when knocking down solely S1P5, indicative of S1P5 activation being responsible for delayed OPC migration.[51] Possibly, S1P3 modulation by P-FTY720 could be responsible for the decrease in OPC migration upon P-FTY720 treatment, depending on which G-protein would be predominantly coupled (Giα, G12/13, and/or Gq).[14] Moreover, P-FTY720 has additional targets and is known to inhibit several cell migration mediators, cadherin, vimentin, matrix metalloproteinases (MMPs), and tissue inhibitor of MMPs.[52]

In summary, our results reveal that the S1P1-selective modulator ponesimod can induce remyelination in an animal model for remyelination. Ponesimod restored demyelination-induced deficits in working memory and reduced the latency time of VEPs in the cuprizone model. Accordingly, ponesimod restored myelination in the medial corpus callosum as assessed with an MBP staining and TEM. The remyelination-inducing effect is at least partially mediated via boosting OPC differentiation.

AUTHOR CONTRIBUTIONS

Emily Willems, Melissa Schepers, Elisabeth Piccart, and Esther Wolfs performed the research and analyzed the data. Emily Willems, Melissa Schepers, and Tim Vanmierlo wrote the manuscript. Maria Ait-Tihyaty, Melissa Schepers, Niels Hellings, and Tim Vanmierlo conceived the research design.

ACKNOWLEDGMENTS

The authors thank Rewind Therapeutics for providing the visual evoked potential equipment.

FUNDING INFORMATION

Research funding was provided by Janssen Research & Development to Tim Vanmierlo.

DISCLOSURES

Author Maria Ait-Tihyaty is an employee of Janssen Pharmaceuticals and may hold stock or stock options in Johnson & Johnson. The authors declare no further competing interests.

DATA AVAILABILITY STATEMENT

The data that support the findings of this study are available in the methods, results, and supplementary material of this article.

ORCID

Emily Willems https://orcid.org/0000-0001-7725-2896
Melissa Schepers https://orcid.org/0000-0001-8090-8489
Esther Wolfs https://orcid.org/0000-0001-9277-6524
Niels Hellings https://orcid.org/0000-0003-2308-406X
Tim Vanmierlo https://orcid.org/0000-0003-2912-0578

REFERENCES

1. Walton C, King R, Rechtman L, et al. Rising prevalence of multiple sclerosis worldwide: insights from the Atlas of MS, third edition. *Mult Scler*. 2020;26(14):1816-1821.
2. Browne P, Chandraratna D, Angood C, et al. Atlas of multiple sclerosis 2013: a growing global problem with widespread inequity. *Neurology*. 2014;83(11):1022-1024.
3. Weiner HL. The challenge of multiple sclerosis: how do we cure a chronic heterogeneous disease? *Ann Neurol*. 2009;65(3):239-248.
4. Chun J, Hla T, Lynch KR, Spiegel S, Moolenaar WH. International Union of Basic and Clinical Pharmacology. LXXVIII. Lysophospholipid receptor nomenclature. *Pharmacol Rev*. 2010;62(4):579-587.
5. Chiba K. FTY720, a new class of immunomodulator, inhibits lymphocyte egress from secondary lymphoid tissues and thymus by agonistic activity at sphingosine 1-phosphate receptors. *Pharmacol Ther*. 2005;108(3):308-319.
6. Kappos L, Bar-Or A, Cree BAC, et al. Siponimod versus placebo in secondary progressive multiple sclerosis (EXPAND): a double-blind, randomised, phase 3 study. *Lancet*. 2018;391(10127):1263-1273.
7. Al-Salama ZT. Siponimod: first global approval. *Drugs*. 2019;79(9):1009-1015.
8. Lamb YN. Ozanimod: first approval. *Drugs*. 2020;80(8):841-848.
9. Comi G, Kappos L, Selmaj KW, et al. Safety and efficacy of ozanimod versus interferon beta-1a in relapsing multiple sclerosis (SUNBEAM): a multicentre, randomised, minimum 12-month, phase 3 trial. *Lancet Neurol*. 2019;18(11):1009-1020.
10. Coret F, Perez-Miralles FC, Gascon F, et al. Onset of secondary progressive multiple sclerosis is not influenced by current relapsing multiple sclerosis therapies. *Mult Scler J Exp Transl Clin*. 2018;4(2):2055217318783347.
11. Sim FJ, Zhao C, Penderis J, Franklin RJ. The age-related decrease in CNS remyelination efficiency is attributable to an impairment of both oligodendrocyte progenitor recruitment and differentiation. *J Neurosci*. 2002;22(7):2451-2459.
12. Nait-Oumesmar B, Decker L, Lachapelle F, Avellana-Adalid V, Bachelin C, Baron-Van Evercooren A. Progenitor cells of the adult mouse subventricular zone proliferate, migrate and differentiate into oligodendrocytes after demyelination. *Eur J Neurosci*. 1999;11(12):4357-4366.
13. Kuhlmann T, Miron V, Cui Q, Wegner C, Antel J, Bruck W. Differentiation block of oligodendroglial progenitor cells as a cause for remyelination failure in chronic multiple sclerosis. *Brain*. 2008;131(Pt 7):1749-1758.
14. Roggeri A, Schepers M, Tiane A, et al. Sphingosine-1-phosphate receptor modulators and oligodendroglial cells: beyond immunomodulation. *Int J Mol Sci*. 2020;21(20):7537.
15. Dietrich M, Hecker C, Martin E, et al. Increased remyelination and proregenerative microglia under siponimod therapy in mechanistic models. *Neurol Neuroimmunol Neuroinflamm*. 2022;9(3):e1161.
16. Ziser L, Meyer-Schell N, Kurniawan ND, et al. Utility of gradient recalled echo magnetic resonance imaging for the study of myelination in cuprizone mice treated with fingolimod. *NMR Biomed*. 2018;31(3).
17. Alme MN, Nystad AE, Bo L, et al. Fingolimod does not enhance cerebellar remyelination in the cuprizone model. *J Neuroimmunol*. 2015;285:180-186.
18. Nystad AE, Lereim RR, Wergeland S, et al. Fingolimod downregulates brain sphingosine-1-phosphate receptor 1 levels but does not promote remyelination or neuroprotection in the cuprizone model. *J Neuroimmunol*. 2020;339:577091.
19. Selkirk JV, Dines KC, Yan YG, et al. Deconstructing the pharmacological contribution of sphingosine-1 phosphate receptors to mouse models of multiple sclerosis using the species selectivity of Ozanimod, a dual modulator of human sphingosine 1-phosphate receptor subtypes 1 and 5. *J Pharmacol Exp Ther*. 2021;379(3):386-399.
20. Kappos L, Fox RJ, Burcklen M, et al. Ponesimod compared with teriflunomide in patients with relapsing multiple sclerosis in the active-comparator phase 3 OPTIMUM study: a randomized clinical trial. *JAMA Neurol*. 2021;78(5):558-567.
21. Kihara Y, Jonnalagadda D, Zhu Y, et al. Ponesimod inhibits astrocyte-mediated neuroinflammation and protects against cingulum demyelination via S1P(1)-selective modulation. *FASEB J*. 2022;36(2):e22132.
22. Schepers M, Paes D, Tiane A, et al. Selective PDE4 subtype inhibition provides new opportunities to intervene in neuroinflammatory versus myelin damaging hallmarks of multiple sclerosis. *Brain Behav Immun*. 2023;109:1-22.
23. Tiane A, Schepers M, Riemens R, et al. DNA methylation regulates the expression of the negative transcriptional regulators ID2 and ID4 during OPC differentiation. *Cell Mol Life Sci*. 2021;78(19–20):6631-6644.
24. Ong W, Lin J, Bechler ME, et al. Microfiber drug/gene delivery platform for study of myelination. *Acta Biomater*. 2018;75:152-160.
25. Frost EE, Milner R, Ffrench-Constant C. Migration assays for oligodendrocyte precursor cells. *Methods Mol Biol*. 2000;139:265-278.
26. Benedict RHB, Tomic D, Cree BA, et al. Siponimod and cognition in secondary progressive multiple sclerosis: EXPAND secondary analyses. *Neurology*. 2021;96(3):e376-e386.
27. DeLuca J, Schippling S, Montalban X, et al. Effect of ozanimod on symbol digit modalities test performance in relapsing MS. *Mult Scler Relat Disord*. 2021;48:102673.
28. Squillace S, Niehoff ML, Doyle TM, et al. Sphingosine-1-phosphate receptor 1 activation in the central nervous system drives cisplatin-induced cognitive impairment. *J Clin Invest*. 2022;132(17):e157738.
29. Doshi A, Chataway J. Multiple sclerosis, a treatable disease. *Clin Med (Lond)*. 2016;16(Suppl 6):s53-s59.
30. Liu M, Duggan J, Salt TE, Cordeiro MF. Dendritic changes in visual pathways in glaucoma and other neurodegenerative conditions. *Exp Eye Res*. 2011;92(4):244-250.

31. Marenna S, Huang SC, Dalla Costa G, et al. Visual evoked potentials to monitor myelin cuprizone-induced functional changes. *Front Neurosci*. 2022;16:820155.
32. Lindner M, Heine S, Haastert K, et al. Sequential myelin protein expression during remyelination reveals fast and efficient repair after central nervous system demyelination. *Neuropathol Appl Neurobiol*. 2008;34(1):105-114.
33. Rockville M. Guidance for industry: estimating the maximum safe starting dose in adult healthy volunteer. U.S. Department of Health and Human Services, Food and Drug Administration, Center for Drug Evaluation and Research (CDER); 2005 Jul. 30 p.
34. Brossard P, Derendorf H, Xu J, Maatouk H, Halabi A, Dingemanse J. Pharmacokinetics and pharmacodynamics of ponesimod, a selective S1P1 receptor modulator, in the first-in-human study. *Br J Clin Pharmacol*. 2013;76(6):888-896.
35. Safaeinejad F, Asadi S, Ghafghazi S, Niknejad H. The synergistic anti-apoptosis effects of amniotic epithelial stem cell conditioned medium and ponesimod on the oligodendrocyte cells. *Front Pharmacol*. 2021;12:691099.
36. Dukala DE, Soliven B. S1P1 deletion in oligodendroglial lineage cells: effect on differentiation and myelination. *Glia*. 2016;64(4):570-582.
37. Keilhauer G, Meier DH, Kuhlmann-Krieg S, Nieke J, Schachner M. Astrocytes support incomplete differentiation of an oligodendrocyte precursor cell. *EMBO J*. 1985;4(10):2499-2504.
38. Reynolds R, Hardy R. Oligodendroglial progenitors labeled with the O4 antibody persist in the adult rat cerebral cortex in vivo. *J Neurosci Res*. 1997;47(5):455-470.
39. Nishiyama A, Chang A, Trapp BD. NG2+ glial cells: a novel glial cell population in the adult brain. *J Neuropathol Exp Neurol*. 1999;58(11):1113-1124.
40. Dawson MR, Polito A, Levine JM, Reynolds R. NG2-expressing glial progenitor cells: an abundant and widespread population of cycling cells in the adult rat CNS. *Mol Cell Neurosci*. 2003;24(2):476-488.
41. Watts VJ, Neve KA. Sensitization of adenylate cyclase by Galpha i/o-coupled receptors. *Pharmacol Ther*. 2005;106(3):405-421.
42. Raible DW, McMorris FA. Cyclic AMP regulates the rate of differentiation of oligodendrocytes without changing the lineage commitment of their progenitors. *Dev Biol*. 1989;133(2):437-446.
43. Verzijl D, Peters SL, Alewijnse AE. Sphingosine-1-phosphate receptors: zooming in on ligand-induced intracellular trafficking and its functional implications. *Mol Cells*. 2010;29(2):99-104.
44. Simon K, Hennen S, Merten N, et al. The orphan G protein-coupled receptor GPR17 negatively regulates oligodendrocyte differentiation via galphai/o and its downstream effector molecules. *J Biol Chem*. 2016;291(2):705-718.
45. Suo N, Guo YE, He B, Gu H, Xie X. Inhibition of MAPK/ERK pathway promotes oligodendrocytes generation and recovery of demyelinating diseases. *Glia*. 2019;67(7):1320-1332.
46. Jaillard C, Harrison S, Stankoff B, et al. Edg8/S1P5: an oligodendroglial receptor with dual function on process retraction and cell survival. *J Neurosci*. 2005;25(6):1459-1469.
47. Novgorodov AS, El-Alwani M, Bielawski J, Obeid LM, Gudz TI. Activation of sphingosine-1-phosphate receptor S1P5 inhibits oligodendrocyte progenitor migration. *FASEB J*. 2007;21(7):1503-1514.
48. Bai A, Shanmugasundaram V, Selkirk JV, Surapaneni S, Dalvie D. Investigation into MAO B-mediated formation of CC112273, a major circulating metabolite of ozanimod, in humans and preclinical species: stereospecific oxidative deamination of (S)-enantiomer of Indaneamine (RP101075) by MAO B. *Drug Metab Dispos*. 2021;49(8):601-609.
49. Tran JQ, Zhang P, Walker S, et al. Multiple-dose pharmacokinetics of ozanimod and its major active metabolites and the pharmacodynamic and pharmacokinetic interactions with pseudoephedrine, a sympathomimetic agent, in healthy subjects. *Adv Ther*. 2020;37(12):4944-4958.
50. Tran JQ, Zhang P, Ghosh A, et al. Single-dose pharmacokinetics of ozanimod and its major active metabolites alone and in combination with gemfibrozil, itraconazole, or rifampin in healthy subjects: a randomized, parallel-group, open-label study. *Adv Ther*. 2020;37(10):4381-4395.
51. Healy LM, Antel JP. Sphingosine-1-phosphate receptors in the central nervous and immune systems. *Curr Drug Targets*. 2016;17(16):1841-1850.
52. White C, Alshaker H, Cooper C, Winkler M, Pchejetski D. The emerging role of FTY720 (fingolimod) in cancer treatment. *Oncotarget*. 2016;7(17):23106-23127.

SUPPORTING INFORMATION

Additional supporting information can be found online in the Supporting Information section at the end of this article.

How to cite this article: Willems E, Schepers M, Piccart E, et al. The sphingosine-1-phosphate receptor 1 modulator ponesimod repairs cuprizone-induced demyelination and induces oligodendrocyte differentiation. *The FASEB Journal*. 2024;38:e23413. doi:10.1096/fj.202301557RR